International Journal of Research and Technology in Electrical Industry

journal homepage: ijrtei.sbu.ac.ir

Shahid Beheshti University

A Planning Framework for Hybrid AC/DC Distribution Networks Considering Heterogeneous Demand Response Characteristics

Lida Yazdani[1] , Mohammad Sadegh Sepasian[1,*] , Hamid Reza Arasteh[2]

[1] *Faculty of Electrical Engineering, Shahid Beheshti University, Tehran, Iran*
[2] *Power Systems Operation and Planning Research Department, Niroo Research Institute, Tehran, Iran 2, Center for Renewable Energy and Microgrid, Huanjiang Laboratory, Zhejiang University, Zhejiang, 311816 China2*

ARTICLE INFO

Article history:
Received: 14 February 2026
Revised: 22 May 2026
Accepted: 30 May 2026

Keywords:
Demand response
Expansion planning
Hybrid AC/DC distribution networks
Load flexibility
Renewable energy sources
Voltage source converter (VSC)

ABSTRACT

Hybrid AC/DC distribution networks (HDNs) have emerged as a promising architecture for integrating distributed energy resources and the growing number of DC loads. However, most existing expansion planning studies treat demand response (DR) as a homogeneous flexibility resource, neglecting the different flexibility characteristics of AC and DC loads. This simplification may lead to unrealistic estimations of demand-side flexibility and suboptimal planning decisions. This paper proposes an expansion planning framework for HDNs that incorporates differentiated DR modelling for AC and DC loads. In the proposed approach, distinct flexibility limits and participation costs are assigned to AC and DC loads to better represent their controllability characteristics. The planning problem is formulated as a mixed-integer nonlinear optimization model that determines network expansion decisions by incorporating DR utilization. The model is solved using a genetic algorithm implemented in MATLAB, while operational costs are evaluated through an optimal power flow module developed in GAMS. Three planning scenarios are analysed to assess the effectiveness of the proposed framework: without DR, with uniform DR, and with differentiated DR for AC and DC loads. The results show that modelling differentiated DR improves demand-side participation and reduces the net present value of total planning costs compared with conventional uniform DR modelling. These findings highlight the importance of accurately representing heterogeneous demand flexibility in the planning of HDNs.

1. Introduction

The increasing penetration of distributed energy resources (DERs), particularly renewable energy sources such as photovoltaic (PV) panels and wind turbines, is fundamentally reshaping the operational paradigm of distribution systems. In parallel, the rapid growth of DC-based loads—including data centers, electric vehicle (EV) chargers, and smart appliances—has accelerated the development of hybrid AC/DC distribution networks (HDNs). These networks offer enhanced energy efficiency, improved voltage regulation, and seamless integration of DC technologies [1–3].

To accommodate these emerging architectures, conventional distribution network expansion planning (DNEP) frameworks must be revisited. Existing studies have investigated HDN expansion through converter-oriented planning strategies [4], strategic allocation of DERs [5], and energy storage system planning [6]. Although these approaches effectively reduce power

* Corresponding author
E-mail address: m_sepasian@sbu.ac.ir
https://orcid.org/0000-0002-6907-0555
https://doi.org/10.48308/ijrtei.2026.243536.1111

losses and improve voltage profiles, they predominantly focus on supply-side flexibility and largely overlook the role of demand-side resources, particularly demand response (DR).

Demand response has emerged as a key flexibility mechanism for peak load mitigation, enhancement of operational security, and deferral of costly network reinforcements [7], [8]. In conventional AC distribution systems, various DR schemes—including price-based programs [9], incentive-based mechanisms [10], and hybrid approaches—have been incorporated into DNEP. However, these models typically assume uniform flexibility or rely on aggregated DR representations to simplify the optimization process.

In hybrid AC/DC distribution networks, DR remains relatively underexplored. Most existing studies either neglect DR entirely or model it as a lumped flexibility resource, disregarding the distinct operational characteristics of AC and DC loads [11]. This simplification fails to capture the higher controllability and faster response of DC loads (such as EV chargers and battery-connected devices) compared to traditional AC residential loads [12], which may lead to suboptimal or unrealistic planning decisions.

To address this research gap, this paper proposes an expansion planning framework for HDNs that explicitly incorporates differentiated DR modeling for AC and DC loads. Distinct flexibility bounds and cost parameters are assigned to each load type, enabling a more realistic representation of demand-side flexibility. The planning process is conducted under peak load conditions, where flexibility provides maximum value, and its robustness is further evaluated using probabilistic operating scenarios generated via Monte Carlo simulation and reduced using the SCENRED toolbox. The results demonstrate that disaggregated DR modelling enhances investment decision-making and improves supply–demand coordination, particularly in networks with high DER penetration.

The main contributions of this study are summarized as follows:

- Development of an HDN expansion planning framework that explicitly incorporates differentiated DR modelling for AC and DC loads, moving beyond conventional aggregated representations.
- Proposal of a hybrid solution approach combining a genetic algorithm (GA) for network configuration selection with an optimal power flow (OPF) module implemented in GAMS for operational cost evaluation.
- Assessment of operational robustness using a reduced probabilistic scenario set to capture uncertainties in load demand and renewable generation.
- Evaluation of flexibility performance under supply-constrained conditions to examine the resilience of selected network configurations.

2. Literature review

2.1. A. Emergence and Justification of Hybrid AC/DC Distribution Networks

Hybrid AC/DC distribution networks have emerged as an effective architecture for integrating conventional AC infrastructures with DC-based technologies such as PV systems, EV chargers, and battery energy storage units. These networks offer improved energy efficiency, reduced power conversion losses, and enhanced voltage stability [13, 14]. Recent review studies have highlighted the potential of HDNs to increase DER hosting capacity and operational resilience while significantly reducing network losses [15].

2.2. B. Planning Challenges in Hybrid AC/DC Systems

Expansion planning in HDNs requires coordinated decisions regarding AC/DC line configuration, converter placement, and DER integration. Due to uncertainties associated with renewable generation and load demand, many studies have adopted stochastic or probabilistic planning approaches [16, 17], employing multi-scenario or chance-constrained formulations to enhance robustness [18]. Nevertheless, most of these methods remain predominantly supply-side oriented and fail to exploit the flexibility potential of controllable DC loads (such as EV chargers and battery systems) which can substantially improve network adaptability under uncertainty.

2.3. C. Demand Response in Conventional and Hybrid Distribution Systems

In conventional AC systems, DR has been widely recognized as an effective tool for peak load management, reliability enhancement, and deferral of network investments [19, 20]. DR has been incorporated into DNEP models through price-based, incentive-based, and hybrid mechanisms, typically assuming uniform or aggregated load representations for computational tractability [21-23]. In HDNs, however, DR has received limited attention and is often modeled as a lumped resource, neglecting the distinct controllability and response dynamics of DC loads such as EVs and energy storage units [24].

2.4. D. Research Gap and Positioning of the Present Study

Recent studies, such as [25], have introduced flexibility-oriented HDN planning frameworks under uncertainty; however, they do not account for the heterogeneous nature of DR across AC and DC loads. This oversimplification limits the accuracy of planning outcomes and weakens the coordination between demand-side and supply-side resources. To overcome this limitation, the present study proposes an HDN expansion planning framework that explicitly differentiates DR characteristics between AC and DC loads. By assigning load-type-specific flexibility bounds and cost parameters, the proposed model captures the individual operational roles of different load categories. Comparative analyses across three planning scenarios—without DR, with uniform DR, and with differentiated DR—demonstrate that accurate representation of load

heterogeneity significantly improves both economic performance and operational efficiency.

3. Modelling framework for HDN expansion planning

The proposed model determines the optimal configuration of an HDN by minimizing total system cost through integrated investment and operational planning. Formulated as a mixed-integer nonlinear programming (MINLP) problem, it is solved using a Genetic Algorithm (GA) for its capability to handle discrete variables and non-convex search spaces. To capture demand-side flexibility, a differentiated DR framework is embedded, distinguishing the participation of AC and DC loads. This enhances the accuracy of load responsiveness representation and its influence on planning results. The following subsections describe the DR modelling approach, objective function, and main operational constraints.

3.1. Differentiated DR modelling for AC and DC loads

In hybrid AC/DC distribution networks, DR is modelled differently for AC and DC loads to capture their operational characteristics. AC loads are less flexible due to comfort, process, or continuity constraints, while DC loads often offer higher controllability and faster response. For example, EV charging stations allow time-shifting [26], data centers provide short-term flexibility via power capping, workload shifting, and UPS coordination [27], and hydrogen electrolyzers adjust power rapidly to support renewables and ancillary services [28]. Accordingly, DC loads are assigned higher participation limits and lower DR costs than AC loads, reflecting practical flexibility in HDNs.

3.2. Objective functions

The objective of the proposed expansion planning model is to minimize the net present value (NPV) of the total cost of the HDN over the planning horizon. As formulated in (1), the total cost (C_{NPV}) includes both the capital investment cost (C_{INV}) and the discounted sum of annual operating and maintenance (O&M) costs (C_{OM}).

$$F = C_{NPV} = C_{INV} + \sum_{t \in T_p} \frac{C_{OM,t}}{(1+d)^t} \tag{1}$$

The total investment cost, given in (3), includes the costs of distribution lines and voltage source converters (VSCs). The line cost component (C_{Line}) covers both AC and DC lines, whose selection depends on the network configuration. The converter cost (C_{Conv}) represents the installation of VSCs required to ensure AC/DC interoperability, either for connecting loads to buses of different types or interfacing lines and buses with mismatched natures. This configuration-dependent allocation guarantees full integration of components within the hybrid structure.

$$C_{INV} = C_{Line} + C_{Conv} \tag{2}$$

In this study, all converters are assumed to be VSCs, due to their controllability, bidirectional power flow capability, and suitability for hybrid AC/DC distribution environments. The annual operating and maintenance cost is calculated according to (3).

$$C_{OM,t} = 8760\, C_{OPF,t} + \beta_M\, C_{INV} \tag{3}$$

To evaluate $C_{OPF,t}$, an OPF analysis is conducted for hour t. The cost includes two components: the energy supply cost from available sources (e.g., upstream grid, DERs), and the cost of implementing DR, as shown in (4).

$$C_{OPF,t} = C_{ENERGY,t} + C_{DR,t} \tag{4}$$

The DR cost ($C_{DR,t}$) is computed in (5) as the sum of curtailed energy from AC and DC loads, multiplied by their respective DR cost coefficients:

$$C_{DR,t} = \sum_{n \in \Omega_b} DR_{n,t}^{AC} \cdot c_n^{AC} + DR_{n,t}^{DC} \cdot c_n^{DC} \tag{5}$$

The model considers a single horizon year under peak load conditions to capture the most stressed scenario, where DR flexibility is most valuable and network reliability is critical.

3.3. Constraints

The constraints governing the HDN expansion planning model are summarized below. These constraints ensure technical feasibility and consistency between investment decisions and network operation.

1) Integer Constraints: This group specifies the binary variables defining the HDN structure (bus types, line connections, and line types) along with their description and values in Table I.

$$MW_n \ , \ MU_{n,m} \ , \ MD_{n,m} \in \{0,1\} \quad \forall n,m \in \Omega_b \tag{6}$$

The binary constraints (6) enable the model to represent a feasible hybrid network configuration in terms of both topology and technology.

2) Bus Connectivity Constraint: This constraint limits the number of lines connected to each bus to maintain network stability and reliability, as expressed in (7). For radial configurations, the total number of lines must be one less than the number of buses, as in (8), ensuring a radial network topology.

$$N_{l,n}^{\min} \le \sum_{\substack{m \in \Omega_b \\ m \ne n}} MU_{nm} \le N_{l,n}^{\max} \ , \quad \forall n \in \Omega_b \tag{7}$$

$$\sum_{n \in \Omega_b} \sum_{\substack{m \in N_b \\ m > n}} MU_{nm} = N_b - 1 \tag{8}$$

Table I. Definition of binary configuration variables.

Variable	Description	Values
MW_n	Bus type indicator (0 for AC, 1 for DC)	0, 1
$MU_{n,m}$	Connection status between bus *n* and *m*	0, 1
$MD_{n,m}$	Line type (0 for AC line, 1 for DC line)	0, 1

3) OPF Constraints: Within the HDN planning formulation, these requirements are classified into four categories, as detailed below:

• Power Balance Constraints: Equations (9) and (10) ensure that injected active and reactive power at each bus equals the demand plus losses, considering the AC/DC nature of lines and buses. The detailed formulation for various AC/DC configurations is presented in [29].

$$P_n^{inj} = P_n^{cal} \quad , \quad \forall n \in \Omega_b \tag{9}$$

$$Q_n^{inj} = Q_n^{cal} \quad , \quad \forall n \in \Omega_b \tag{10}$$

• Network Constraints: The constraints (11)-(13) define the operational limits for voltage magnitudes, voltage phase angles, and power flows across the network, ensuring that all variables remain within technically permissible ranges.

$$V_n^{\min} \le V_n \le V_n^{\max} \quad , \quad \forall n \in \Omega_b \tag{11}$$

$$\theta_n^{\min} \le \theta_n \le \theta_n^{\max} \quad , \quad \forall n \in \Omega_b \tag{12}$$

$$\sqrt{P_{nm}^2 + Q_{nm}^2} \le S_{nm}^{\max} \quad , \quad \forall n,m \in \Omega_b \tag{13}$$

• Converter Constraints: Converter Constraints: Each VSC must satisfy the apparent power and modulation index limits, as defined in (14) and (15), ensuring feasible and stable converter operation.

$$\sqrt{P_c^2 + Q_c^2} \le S_c^{\max} \quad , \quad \forall c \in \Omega_c \tag{14}$$

$$M_{c(nm)}^{\min} \le M_{c(nm)} \le M_{c(nm)}^{\max} \quad , \quad \forall n,m \in \Omega_b \tag{15}$$

• Generator Constraints: To maintain system reliability and stability, the active and reactive power outputs of AC generators and the active power of DC sources are restricted within their allowable limits, as formulated in (16)– (18).

$$P_{G_i}^{ac,\min} \le P_{G_i}^{ac} \le P_{G_i}^{ac,\max} \quad , \quad \forall i \in \Omega_i \tag{16}$$

$$Q_{G_{i1}}^{ac,\min} \le Q_{G_i}^{ac} \le Q_{G_i}^{ac,\max} \quad , \quad \forall i \in \Omega_i \tag{17}$$

$$P_{G_{id}}^{dc,\min} \le P_{G_{id}}^{dc} \le P_{G_{id}}^{dc,\max} \quad , \quad \forall id \in \Omega_{id} \tag{18}$$

4) DR Constraints: These constraints limit demand reductions within the predefined flexibility bounds for each load type, ensuring that the economic and technical characteristics of AC and DC demands are properly represented, as expressed in (19) and (20).

$$0 \le DR_{n,t}^{AC} \le K_{n,t}^{AC} \quad , \quad \forall n \in \Omega_b \tag{19}$$

$$0 \le DR_{n,t}^{DC} \le K_{n,t}^{DC} \quad , \quad \forall n \in \Omega_b \tag{20}$$

3.4. Modelling Assumptions

- The locations and maximum demand of AC and DC loads, as well as the capacities of distributed generation (DG) units, are assumed to be known in advance. The planning problem therefore focuses on determining the optimal network configuration, including the AC/DC type of buses, the AC/DC type and routing of distribution lines, and the number and placement of AC/DC converters
- The planning problem is formulated as a MINLP and solved using DICOPT/CONOPT4 to capture nonlinear AC–DC interactions.
- The planning stage is performed under peak-load conditions.
- Uncertainty in renewable generation is modelled using Monte Carlo simulation and scenario reduction via SCENRED for performance evaluation.
- The hybrid AC/DC network is represented using the unified load-flow model adopted from [29].
- All AC/DC interfaces are assumed to be VSC-based converters.
- Renewable DGs operate under a FIT scheme with fixed generation costs based on [30].

4. Planning methodology

To determine the optimal expansion strategy for HDNs while accounting for differentiated DR, a two-level methodology is developed. As illustrated in Fig. 1, the planning framework combines a GA with a DR-based OPF module to iteratively search for cost-effective and operationally feasible HDN configurations. The GA module is responsible for exploring topological alternatives through binary-encoded configuration matrices, while the OPF module evaluates each candidate solution by solving the operational subproblem under peak load conditions. This integrated framework enables the identification of HDN configurations that minimize total planning costs while considering both investment and operation under flexibility constraints. The following section outlines the flowchart, accompanied by explanations of each stage to improve clarity.

Step 1 – Chromosome Initialization

A set of candidate chromosomes is created randomly. Each chromosome is a binary-encoded structure that determines the network configuration through three matrices MW, MU, and MD. Based on these matrices, the location and number of VSCs are implicitly

identified by the need to interface AC and DC subsystems.

Step 2 – Network Connectivity Check

Each chromosome is examined to ensure that the resulting network is connected and feasible from a topological perspective. Configurations that result in isolated buses or unreachable loads are discarded.

Step 3 – Radiality Check

The resulting connected network is further examined to ensure it satisfies the radial topology requirement, as formally defined by Constraint (8) in the model formulation. Configurations that violate this radiality constraint—such as those containing loops or meshed segments—are considered infeasible and excluded from further evaluation.

Step 4 – DR-Based OPF Module (GAMS Implementation)

For each valid chromosome, an OPF problem is solved under peak load conditions using GAMS. The OPF minimizes the operational cost, which includes:

- Energy purchase from upstream grid and local DERs
- DR participation costs, with differentiated modelling for AC and DC loads.

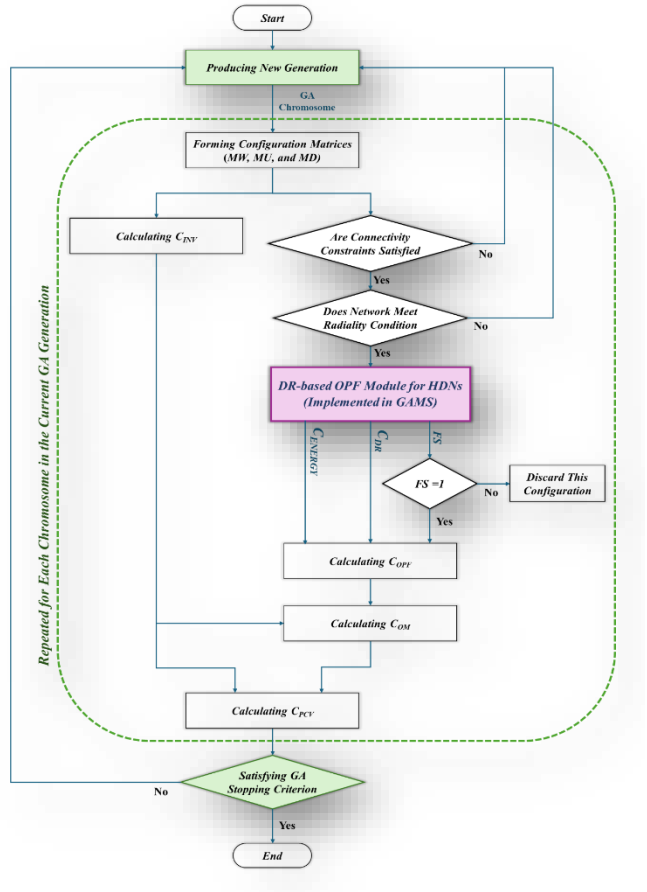

Fig. 1. Flowchart of the proposed GA-based planning model for HDN development incorporating differentiated.

The OPF module solves the power flow problem while satisfying all relevant technical constraints, including power balance, network, converter, generator, and DR constraints, as defined in (9)-(20).

Step 5 – Cost Evaluation

The NPV of each configuration is calculated by summing:

- Investment costs (lines and converters),
- Discounted annual operational costs obtained from the OPF

This NPV acts as the fitness value for each chromosome in the GA population.

Step 6 – GA Operators (Selection, Crossover, Mutation)

Using fitness-based selection, parent chromosomes are chosen to create a new generation through crossover and mutation. These operations introduce diversity and guide the population toward better solutions.

Step 7 – Convergence Check

The process iterates until the stopping condition is met— a convergence threshold on the best NPV. If the condition is not satisfied, the algorithm returns to Step 1.

Step 8 – Output the Optimal Configuration

Once convergence is achieved, the best-performing chromosome is selected as the final solution. This chromosome represents the optimal HDN configuration with corresponding DR participation strategies, DER integration, and converter placements.

In summary, the proposed methodology integrates topology optimization and operational assessment within a unified planning framework. By combining GA-based configuration search with OPF analysis under peak conditions, the model effectively captures the technical and economic impacts of differentiated DR. This ensures that the resulting HDN plan is both cost-efficient and operationally robust.

Table II. Thirteen-area test system — reported load figures reflect peak consumption and DG values refer to maximum available capacity

		Zone 4: - PV DG: 1.5 MW - AC load: 0.5 MW and 0.25 MVAR		***Zone 9:*** - Wind DG:1.0 MW - DC load: 0.85 MW	
	Zone 2: -AC load: 1.0 MW and 0.45 MVAR		***Zone 7:*** - PV DG: 1.5 MW - AC load: 0.5 MW and 0.25 MVAR		***Zone 12:*** - EV station: 1.25 MW
Zone 1: DSS capacity: 10 MW and 4.8 MVAR		***Zone 5:*** - AC load: 0.5 MW and 0.25 MVAR - DC load: 0.5 MW		***Zone 10:*** - AC load: 0.5 MW and 0.25 MVAR - DC load: 0.5 MW	
	Zone 3: - EV station: 1.25 MW		***Zone 8:*** -EV station: 1.25 MW - AC load: 0.5 MW and 0.25 MVAR		***Zone 13:*** - Diesel DG: 2.0 MW and 0.96 MVAR - AC load: 0.75 MW and 0.35 MVAR
		Zone 6: -AC load: 0.75 MW and 0.35 MVAR - DC load: 0.75 MW		***Zone 11:*** - PV DG:1.5 MW	

Table III. Comparison of DR scenarios in HDN planning

Scenario	DR Included	AC/DC Load Treatment	DR Participation	DR Price Incentive	Description
Scenario 1 (No DR)	No	–	–	–	Reference scenario without DR; used as the baseline for performance comparison.
Scenario 2 (Uniform DR Strategy)	Yes	Treated Equally	Same level for both	Equal for AC & DC	Simplified approach where all loads, regardless of type, respond similarly to DR signals.
Scenario 3 (Differentiated DR Strategy)	Yes	Treated Differently	Higher for DC, lower for AC	Lower for DC loads	Reflects greater responsiveness and efficiency from DC loads by offering stronger incentives.

5. Simulation results and discussion

5.1. System description

To evaluate the effectiveness of the proposed HDN expansion planning framework, a 13-zone hybrid distribution network is adopted as the case study. Each zone, modelled as a single bus, can be configured as AC or DC depending on optimization results, with Bus 1 connected to the utility grid through the Distribution System Service (DSS) model. Network lines may also adopt either AC or DC configurations; DC lines follow a unipolar layout, suitable for medium-voltage hybrid systems due to their simplicity and lower cost.

Each zone hosts AC/DC loads, distributed generators (PV, wind, and diesel), and EV charging stations, with detailed capacities listed in Table II. The complete AC and DC load demands at each bus are provided in Appendix A, Table A.1, and the full data for all generators (type, and capacity limits) are given in Appendix A, Table A.2. A symmetric distance matrix *Dis* described in [25] represents inter-zone distances for estimating line installation costs. Nominal voltages are 4.16 kV (AC) and 6.8 kV (DC). Renewable DGs operate under the Feed-in-Tariff (FIT) scheme with generation costs of 209 $/MWh for PV and 128 $/MWh for wind, while grid or diesel power costs 92.2 $/MWh [30].

During OPF analysis, voltage magnitudes are constrained within 0.95–1.05 p.u., and phase angles within $\pm\pi/4$ rad. All lines use AWG#4/0 ACSR conductors with a 2 MVA thermal limit and installation cost of 28 k$/mile [31]. Voltage Source Converters (VSCs) linking AC and DC sections operate at 95% efficiency, a modulation index of 0.77–1.0, and an installation cost of 170 $/kVA [25]; annual maintenance is set at 5% of investment cost.

Table IV. Comparison of simulation results across DR integration scenarios in HDNs

	Parameter	Scenario 1	Scenario 2	Scenario 3
Economic Performance	C_{INV} (M$)	2.1669	2.5685	2.5125
	C_{OPE} (M$)	4.7844	4.1650	4.0954
	C_{NPV} (M$)	6.9513	6.7335	6.6079
DR participation	Average DR Participation Rate [%]	–	6.4	10.8
	AC Load DR Participation [%]	–	4.5	4.5
	DC Load DR Participation [%]	–	7.9	15.8
Network Configuration	Number of AC Buses	6	6	6
	Number of DC Buses	7	7	7
	Number of AC Lines	6	5	5
	Number of DC Lines	6	7	7
	Number of VSCs between Lines and Buses	3	3	3
Technical Behavior	Power Losses [%]	4.7	6.2	6.6

5.2. *Evaluation of the proposed DR strategy in HDN system planning*

Before presenting the comparative results of the three planning scenarios, it is noted that the obtained configuration corresponds to the best feasible solution identified by the GA-based main problem after structural screening through connectivity and radiality checks. For each structurally valid configuration, the OPF-based subproblem is solved in GAMS using DICOPT and CONOPT4 to ensure full satisfaction of operational and technical constraints. Therefore, the configuration reported in this section has passed both structural and operational validation. Its performance is then assessed in the following subsections through deterministic scenario comparison (Section 5.2), probabilistic robustness evaluation (Section 5.3), and flexibility assessment under supply constraints (Section 5.4).

This subsection presents and discusses the results of the HDN planning model under three distinct scenarios, as summarized in Table III: without DR (Scenario 1), with uniform DR for all loads (Scenario 2), and with differentiated DR based on load type (Scenario 3). Scenario 1 assumes no DR participation, serving as a pure investment-based benchmark. In Scenario 2, a unified DR strategy is applied in which identical cost and participation limits are defined for both AC and DC loads. However, their actual DR participation levels may differ due to network topology and operational constraints. These reference cases are used to provide context for assessing the relative effectiveness of the proposed strategy discussed in Scenario 3.

The results of the HDN planning, evaluated under the three strategies outlined in Table III, are presented in Table IV. A comprehensive comparison is conducted across four key dimensions: 1) economic performance, 2) DR participation, 3) network configuration, and 4) technical behavior. Further analysis of these dimensions is provided in the following subsections.

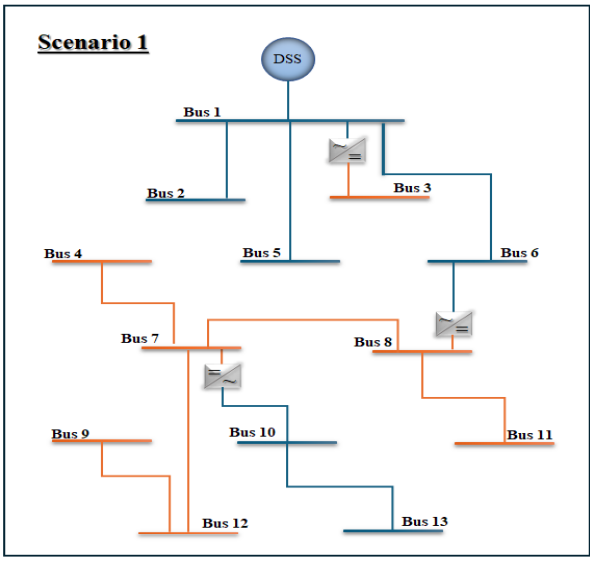

(a)

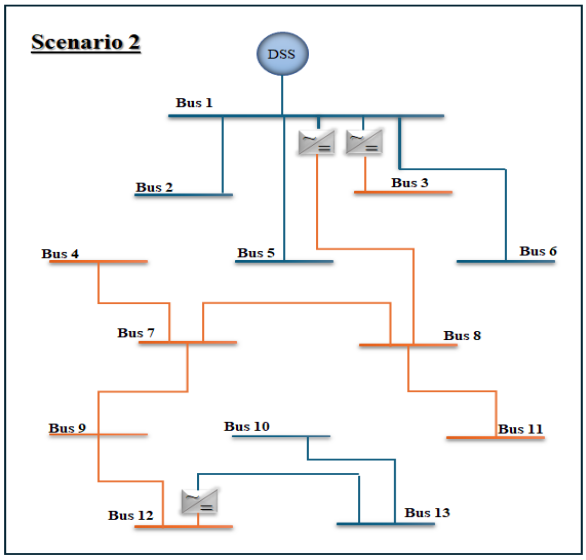

(b)

Fig. 2. Optimal network topologies corresponding to Scenario 1 (without DR) and Scenario 2 (with uniform DR). (a) Network layout for Scenario 1, (b) Network layout for Scenario 2.

1) Economic Performance

Scenario 1 results in the highest total cost due to the absence of flexibility, forcing the planner to rely primarily on infrastructure investment. Introducing uniform DR in Scenario 2 reduces operating expenses but increases investment, as additional network reinforcement is required to accommodate more flexible dispatch patterns.

In Scenario 3, the differentiated DR strategy achieves the minimum total cost with slightly lower investment compared to Scenario 2. This improvement arises from the more effective utilization of load-type-specific flexibility, which allows demand adjustment where it is

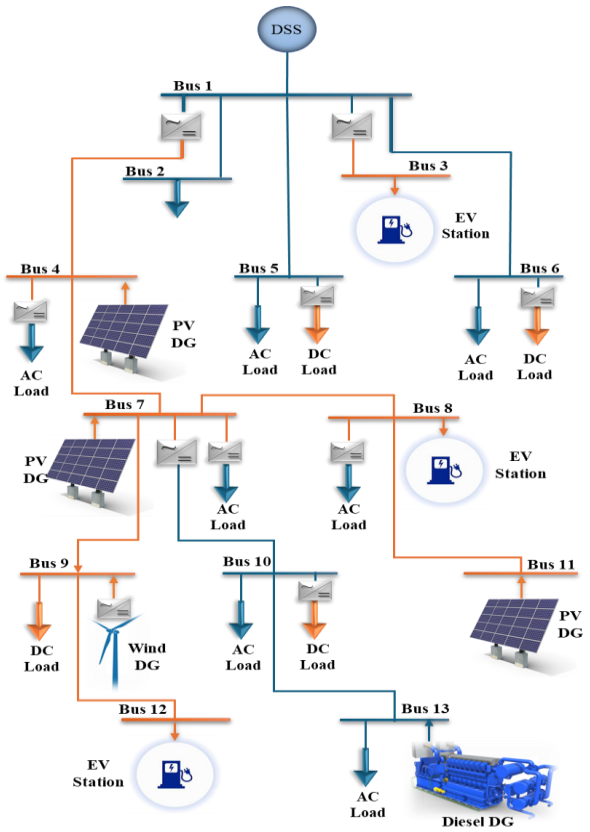

Fig. 3. Final topology derived from the proposed HDN expansion planning framework incorporating differentiated DR (Scenario 3).

technically most efficient rather than uniformly across all buses. Consequently, the planner can reduce costly reinforcements while maintaining operational feasibility. These results indicate that incorporating load heterogeneity into DR modelling leads to economically superior expansion decisions.

2) DR Participation

The average DR participation increases from 6.4% in Scenario 2 to 10.8% in Scenario 3, driven mainly by DC loads (15.8%) compared with AC loads (4.5%). This indicates that the differentiated DR strategy is able to utilize flexible demand more effectively than the uniform scheme. In particular, a larger share of the responsive demand is activated on the DC side, which improves the overall effectiveness of DR deployment in the hybrid network. Therefore, the increase in participation is not merely quantitative, but also reflects a more efficient allocation of flexibility across the system.

3) Network Configuration

Across the three scenarios, the numbers of AC and DC buses remain constant at 6 and 7, respectively, indicating that DR primarily affects line selection rather than node allocation. However, Scenarios 2 and 3 exhibit a higher proportion of DC lines compared to Scenario 1, suggesting a structural tendency toward DC Lines when flexibility is available.

This shift can be explained by the improved compatibility between DC infrastructure and flexible DC loads, which reduces conversion stages and enhances dispatch efficiency. Meanwhile, the number of VSCs remains unchanged at three, as it is determined by

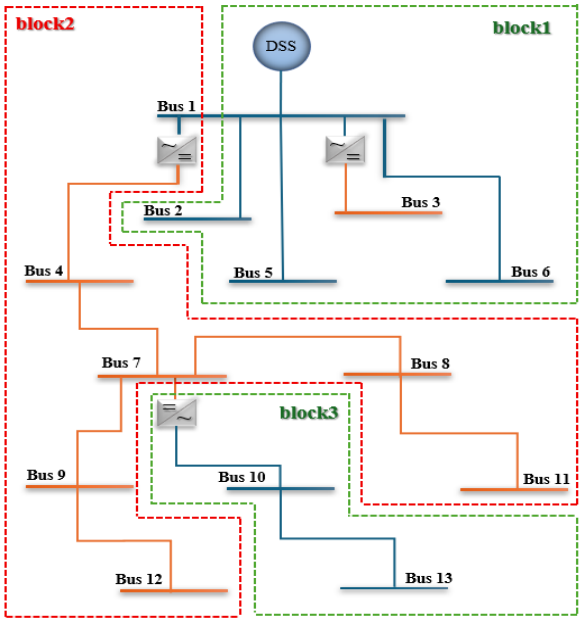

Fig. 4. Block-based partitioning of the optimal HDN topology derived from Scenario 3.

fundamental interconnection requirements rather than operational flexibility. Therefore, DR influences the internal reinforcement pattern of the network without altering its basic AC/DC interface architecture. Fig. 2 illustrates the network topology for Scenarios 1 and 2, while Fig. 3 presents the final topology obtained for Scenario 3 from the proposed HDN expansion framework.

4) Power Losses

As shown in Fig. 4, the network can be divided into three blocks. Blocks 1 and 3 remain structurally unchanged across all scenarios, while Block 2 is reconfigured depending on the DR strategy. In Blocks 1 and 3, loads are located near low-cost AC sources, resulting in minimal DR activation. In contrast, Block 2 is dominated by PV units with relatively higher generation costs, making it economically advantageous to shift part of the demand toward upstream AC sources via DR.

This redistribution increases transmitted power over certain feeders, leading to slightly higher total losses in Scenarios 2 and 3 (6.2% and 6.6%) compared to Scenario 1 (4.7%). However, the additional loss cost is economically offset by reduced generation and operational expenses. This result highlights an important planning insight: marginal increases in technical losses can be acceptable if they enable more cost-efficient resource utilization at the system level.

5) Overall Evaluation

Scenario 3 demonstrates superior performance across economic, operational, and demand participation indicators. By capitalizing on the technical flexibility of DC loads, it facilitates greater and more cost-efficient DR utilization. These findings underscore the value of incorporating differentiated DR strategies during the planning stage, contributing to the development of more resilient and cost-effective hybrid distribution networks.

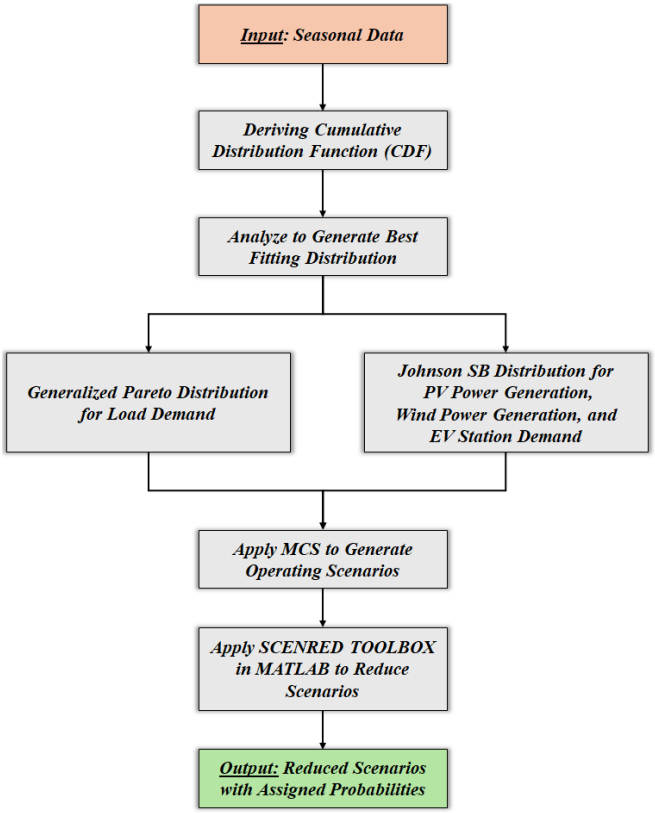

Fig. 5. Flowchart of the operating scenarios generation and reduction process.

5.3. *Operational Robustness Assessment of Scenario 3 Using Probabilistic Scenarios*

To evaluate the robustness of the proposed HDN planning under realistic operating conditions, an operating scenario generation framework is developed, as shown in Fig. 5. The method captures uncertainties in load demand and RESs while maintaining computational efficiency. Seasonal data for AC/DC loads, PV and wind generation, and EV charging demand are collected to construct their cumulative distribution functions (CDFs) and identify suitable probabilistic models. The Generalized Pareto Distribution is used for load demand to represent both normal and extreme variations, while the Johnson SB Distribution models PV, wind, and EV data due to their bounded ranges. The numerical parameters of these probabilistic models are provided in Appendix A, Table A.3.

Monte Carlo Simulation (MCS) generates a large set of operating cases, which is then reduced using the SCENRED toolbox in MATLAB. The reduction algorithm minimizes the Kantorovich distance between the full and reduced sets, yielding a compact scenario tree with assigned probability weights. The resulting set represents the most probable and diverse operating conditions and is used in the OPF analysis of Scenario 3. This approach ensures that system performance is evaluated under realistic stochastic variations with preserved computational tractability.

Table V compares Scenario 3 under peak and probabilistic conditions. While planning is based on peak demand, probabilistic scenarios capture more realistic network states, reducing operating cost and total NPV by 46% and 29%, respectively. Despite lower loading, DR remains effective, confirming its continued contribution to cost efficiency. Average DR participation remains similar across scenarios (10.8% vs. 9.5%), with DC loads showing greater flexibility. These results underscore the robustness of the planned network: even when demand levels are lower than the peak, the inherent flexibility of the system, particularly through DR, continues to yield significant cost savings. The consistency in average DR participation (10.8% vs. 9.5%) between peak and probabilistic cases suggests that the network is not just optimized for a single worst-case point, but possesses a structural flexibility that adapts to stochastic variations.

Table V. comparison of results for scenario 3 under peak load condition and operating scenarios

Category	Parameter	Peak Load	Operating scenarios
Economic Performance	C_{OPE} (M$)	4.0954	2.2093
	C_{NPV} (M$)	6.6079	4.7218
DR participation	Average DR Participation Rate [%]	10.8	9.5
	AC Load DR Participation [%]	4.5	3.8
	DC Load DR Participation [%]	15.8	14.6
Technical Behavior	Power Losses (MW) [%]	6.6	6.4

Fig. 6 depicts the link between DR participation and operating cost: larger bubbles represent higher DR levels associated with lower costs, while warmer colors indicate DC- dominant DR with the highest economic benefit. This visualization highlights that the synergy between DC-side flexibility and network operation is a key driver for robustness. Overall, results confirm that the proposed plan maintains economic robustness under varying operating conditions, proving that the integration of differentiated DR serves as a hedge against demand and RES uncertainties.

5.4. *Flexibility Assessment of the Proposed DR-Based HDN Planning under Supply Constraints*

The robustness of the proposed DR-based HDN planning (Scenario 3) is evaluated under three supply-constrained scenarios: (1) limited upstream import capacity (50% of nominal) to reflect DSO capacity management strategies [32], (2) reduced PV generation (≈20% of nominal) representing low-output conditions due to overcast weather [33], and (3) zero wind output caused by off-range wind speeds [34]. These cases capture realistic operational uncertainties in distribution networks, where the network must rely on its internal flexibility rather than external supply. Following the same economic logic presented in Section 5.2, the proposed differentiated DR strategy is expected to outperform Scenarios 1 and 2 even under supply constraints. Table VI presents the performance of

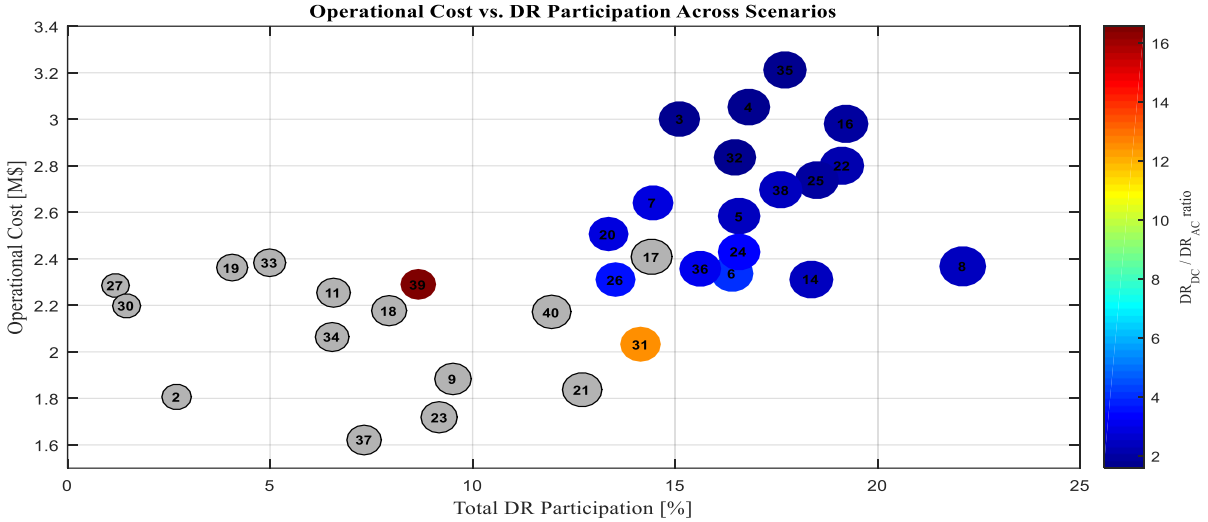

Fig. 6. Bubble chart of DR participation across reduced operating scenarios, where bubble size reflects total DR, color indicates the DR_{DC}/DR_{AC} ratio, and gray bubbles denote cases with DC-only participation. Scenarios with no DR are omitted.

Table VI. System performance under base and three supply-constrained cases based on scenario 3

	Indicator	No Supply Constraints	50% Upstream Limit	PV Generation ~20%	Wind Curtailment
Economic Evaluation [M$]	Net Present Value (NPV)	4.0954	4.6063	4.098	4.2681
	Operational Cost	6.6079	7.1188	6.6105	6.7806
DR Performance [%]	Total DR Participation	10.8	20.3	11.4	15.8
	AC Load DR Participation	4.5	10.9	5.1	9.0
	DC Load DR Participation	15.8	27.6	16.4	21.1
Supply-Side Contribution [MWh]	Energy Supplied by Diesel/Grid	8.8981	6.8020	8.8981	8.8981
	Energy Supplied by PV	0.9313	1.7821	0.7870	1.3191
	Energy Supplied by Wind	1.0000	1.0000	1.0000	0
Reliability [MWh]	Load Reduction via DR	1.2300	2.3015	1.2935	1.7900
	Energy Not Supplied	0	0	0	0
	Total Supplied Load*	10.1200	9.0485	10.0565	9.5600

* Note: In this study, the reported 'Total Supplied Load' represents only the portion of demand that received energy from supply-side resources (PV, wind, diesel, grid). It excludes both demands curtailed by DR and any demand not served due to supply limitations (ENS).

Scenario 3 under normal and supply-constrained conditions, and the results confirm that the proposed strategy avoids ENS and utilizes cheaper DC flexibility, consistent with the economic logic from Section 5.2. Simulation results (Table VI) indicate that the proposed strategy maintains high operational flexibility. Key findings include:

a) High-Flexibility DC Utilization: DC loads provide the main source of flexibility, achieving up to 27.6% DR participation under severe constraints. This confirms that the differential modelling approach (assigned in Section 3.1) allows the system to tap into the most cost-effective and responsive reserve resources precisely when external supply is most compromised.

b) Resilience through DR: Full demand satisfaction is maintained with zero unserved energy, as DR effectively compensates for supply limitations (e.g., 2.3 MWh curtailed via DR in Case 1). This proves that the proposed planning not only optimizes nominal costs but also provides an operational hedge that prevents load shedding during supply outages.

c) Economic Stability: Economic impacts of renewable variability are modest, with only slight increases in NPV, indicating that the differentiated DR strategy successfully absorbs fluctuations. By shifting demand away from periods of low renewable output, the system minimizes reliance on expensive upstream power, thereby insulating the overall NPV from renewable-related volatility.

The radar diagram in Fig. 7 illustrates the performance of Scenario 3 under various supply-side constraints, highlighting that the planning framework creates a robust operational envelope, where the trade-off between economic investment and operational flexibility is optimized to maintain performance even under adverse supply conditions.

6. Conclusion

This study presented a novel expansion planning framework for HDNs that explicitly incorporates differentiated DR modelling for AC and DC loads. By recognizing the distinct flexibility characteristics and incentive requirements of each load type, the proposed approach advances beyond conventional planning methods that assume uniform DR participation. The planning problem was formulated as a mixed-integer nonlinear programming (MINLP) model and solved using a GA in MATLAB, with operational costs evaluated through an OPF module implemented in GAMS under peak load conditions.

Simulation results confirmed that differentiated DR integration improves both economic efficiency and system flexibility. The scenario featuring distinct DR characteristics for AC and DC loads achieved the most cost-effective planning outcome. Further analysis under

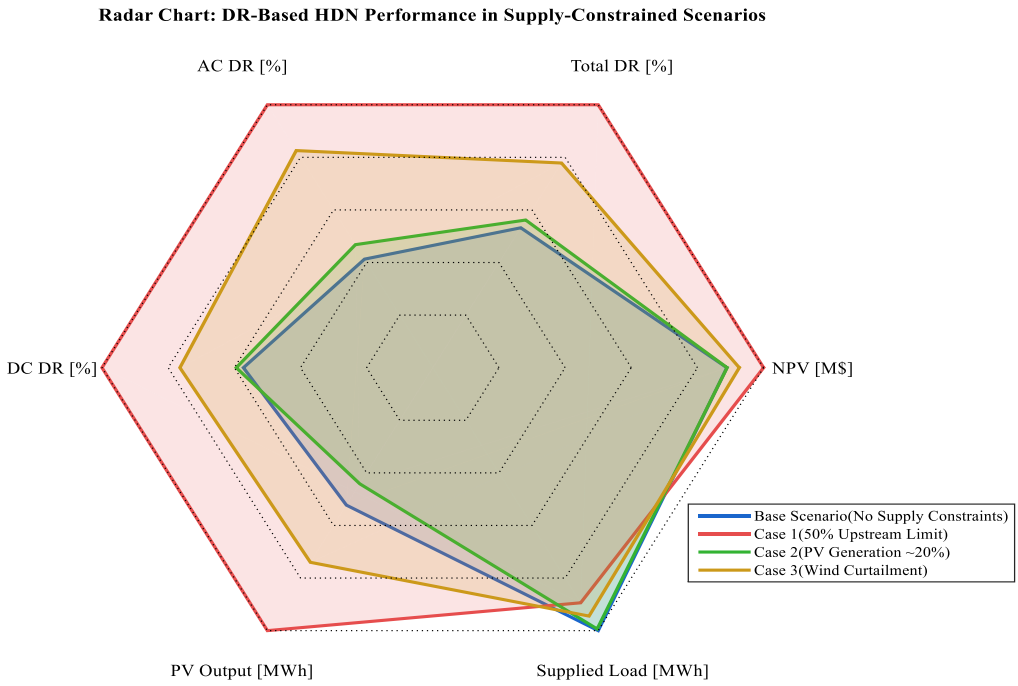

Fig. 7. Multi-criteria evaluation of the proposed DR-based HDN planning strategy (Scenario 3) under supply constraints.

probabilistic operating conditions verified that, although the planning was performed at peak demand, DR—particularly from DC loads—remained effective in reducing operating costs and maintaining operational robustness under realistic uncertainty. Evaluations of supply-side constraints confirmed the resilience and adaptability of the proposed planning strategy. The findings emphasize the vital role of DC-side flexibility in enhancing both reliability and economic performance. The framework is scalable and adaptable to diverse planning environments. Future work will extend the model to include temporal DR shifting, energy storage, and upstream grid interactions to better reflect real-world HDN conditions.

7. References

[1] M. I. Abdelwanis and M. I. Elmezain, "A comprehensive review of hybrid AC/DC networks: insights into system planning, energy management, control, and protection," Neural Computing and Applications, vol. 36, no. 29, pp. 17961–17977, 2024.
[2] Z. Javid, I. Kocar, W. Holderbaum, and U. Karaagac, "Future distribution networks: A review," Energies, vol. 17, no. 8, p. 1822, 2024.
[3] O. Azeem et al., "A comprehensive review on integration challenges, optimization techniques and control strategies of hybrid AC/DC Microgrid," Applied Sciences, vol. 11, no. 14, p. 6242, 2021.
[4] B. Zhang, L. Zhang, W. Tang, G. Li, and C. Wang, "Optimal planning of hybrid AC/DC low-voltage distribution networks considering DC conversion of three-phase four-wire low-voltage AC systems," Journal of Modern Power Systems and Clean Energy, vol. 12, no. 1, pp. 141–153, 2023.
[5] H. Farhangi, "The path of the smart grid," IEEE Power and Energy Magazine, vol. 8, no. 1, pp. 18–28, 2010, doi: 10.1109/MPE.2009.934876.
[6] J. Zhao et al., "Distributed Energy Storage Configuration Method for AC/DC Hybrid Distribution Network Based on Bi-Level Optimization," Batteries, vol. 12, no. 1, p. 9, 2025.
[7] Z. Lu, X. Li, J. Ge, X. Qiu, and X. Zhang, "An Optimization Research of an AC-DC Hybrid Distribution Network with PET Based on Demand Response," in 2025 IEEE 3rd International Conference on Power Science and Technology (ICPST), 2025: IEEE, pp. 1184–1189.
[8] A.-H. Mohsenian-Rad and A. Leon-Garcia, "Optimal residential load control with price prediction in real-time electricity pricing environments," IEEE transactions on Smart Grid, vol. 1, no. 2, pp. 120–133, 2010.
[9] J. Haakana, J. Haapaniemi, O. Räisänen, J. Lassila, J. Partanen, and R. Toivanen, "Will the Spot-Price-Based Demand Response Overload the Distribution Network?," in IET Conference Proceedings CP785, 2021, vol. 2021, no. 6: IET, pp. 2193–2197.
[10] Z. Ding et al., "Optimal Planning of Distribution Network Expansion Considering Integrated Demand Response," in 2021 6th International Conference on Power and Renewable Energy (ICPRE), 2021: IEEE, pp. 776–781.
[11] H. Li, X. Guo, and J. Li, "Power coordination control method for AC/DC hybrid microgrid considering demand response," International Journal of Emerging Electric Power Systems, vol. 26, no. 1, pp. 133–144, 2025.
[12] C.-H. Lin, J.-L. Chen, C.-L. Kuo, and L.-Y. Chang, "Direct Electronic Load Control for Demand Response in a DC Microgrid Using a Virtual Internal Impedance Screening Model and PID Controller," Technology and Economics of Smart Grids and Sustainable Energy, vol. 3, pp. 1–14, 2018.
[13] Y. Guo, S. Wang, and D. Chen, "A Time-and Space-Integrated Expansion Planning Method for AC/DC Hybrid Distribution Networks," Sensors, vol. 25, no. 7, p. 2276, 2025.
[14] H. Lotfi and A. Khodaei, "AC versus DC microgrid planning," IEEE transactions on smart grid, vol. 8, no. 1, pp. 296–304, 2015.
[15] S. J. U. Hassan et al., "Towards medium voltage hybrid AC/DC distribution Systems: Architectural Topologies, planning and operation," International Journal of Electrical Power & Energy Systems, vol. 159, p. 110003, 2024.
[16] H. Doagou‐Mojarrad, H. Rastegar, and G. B. Gharehpetian, "Probabilistic multi‐objective HVDC/AC transmission expansion planning considering distant wind/solar farms," IET Science, Measurement & Technology, vol. 10, no. 2, pp. 140‐149, 2016.
[17] M. Moradi-Sepahvand and T. Amraee, "Hybrid AC/DC transmission expansion planning considering HVAC to HVDC conversion under renewable penetration," IEEE Transactions on Power Systems, vol. 36, no. 1, pp. 579–591, 2020.
[18] S. Camal, F. Teng, A. Michiorri, G. Kariniotakis, and L. Badesa, "Scenario generation of aggregated wind, photovoltaics and small hydro production for power systems applications," Applied Energy, vol. 242, pp. 1396–1406, 2019.
[19] X. Yan, C. Gu, H. Zhang, F. Li, and Y. Song, "Waiting cost based long-run network investment decision-making under uncertainty," IEEE Transactions on Power Systems, vol. 36, no. 4, pp. 3340–3348, 2020.

[20] G. Sivasankari, S. Prasanthini, N. Vijithra, K. Narayanan, G. Sharma, and T. Senjyu, "Reliability enhancement based on demand response for profit maximization," in 2022 2nd International Conference on Power Electronics & IoT Applications in Renewable Energy and its Control (PARC), 2022: IEEE, pp. 1–5.
[21] J. P. Carvallo and L. C. Schwartz, "The use of price-based demand response as a resource in electricity system planning," 2023.
[22] A. Pourramezan and M. Samadi, "A novel approach for incorporating incentive-based and price-based demand response programs in long-term generation investment planning," International Journal of Electrical Power & Energy Systems, vol. 142, p. 108315, 2022.
[23] M. A. Alotaibi and M. M. Salama, "An incentive-based multistage expansion planning model for smart distribution systems," IEEE Transactions on Power Systems, vol. 33, no. 5, pp. 5469–5485, 2018.
[24] M. Kazerani, "A high-performance controllable dc load," in 2007 IEEE International Symposium on Industrial Electronics, 2007: IEEE, pp. 1015–1020.
[25] L. Yazdani, M. S. Sepasian, and H. R. Arasteh, "Optimal comprehensive planning for AC/DC hybrid distribution networks: Balancing cost, risk, and flexibility with variable RES installations," Electric Power Systems Research, vol. 246, p. 111703, 2025.
[26] K. Pan, C.-D. Liang, and M. Lu, "Optimal scheduling of electric vehicle ordered charging and discharging based on improved gravitational search and particle swarm optimization algorithm," International Journal of Electrical Power & Energy Systems, vol. 157, p. 109766, 2024.
[27] D. Al Kez, A. Foley, F. Ahmed, and J. Morrow, "Data Center Potential Flexibilities and Challenges for Demand Response to Facilitate 100% Inverter-Based Resources: A Review," Available at SSRN 4269631, 2022.
[28] J. Eichman, K. Harrison, and M. Peters, "Novel electrolyzer applications: providing more than just hydrogen," National Renewable Energy Lab.(NREL), Golden, CO (United States), 2014.
[29] H. M. Ahmed, A. B. Eltantawy, and M. Salama, "A generalized approach to the load flow analysis of AC–DC hybrid distribution systems," IEEE Transactions on Power Systems, vol. 33, no. 2, pp. 2117–2127, 2017.
[30] H. M. Ahmed, A. B. Eltantawy, and M. M. Salama, "A planning approach for the network configuration of AC-DC hybrid distribution systems," IEEE Transactions on Smart Grid, vol. 9, no. 3, pp. 2203–2213, 2016.
[31] H. M. Ahmed, A. B. Eltantawy, and M. Salama, "A reliability-based stochastic planning framework for AC-DC hybrid smart distribution systems," International Journal of Electrical Power & Energy Systems, vol. 107, pp. 10–18, 2019.
[32] O. Governor's Energy, "DSO Feasibility Study: Draft Results," State of Maine, Governor's Energy Office, Augusta, ME, USA, 2025/06/10 2024. [Online]. Available: https://www.maine.gov/energy/sites/maine.gov.energy/files/meetings/DSO%20draft%20study%20results%20Nov%202024.pdf
[33] T. E. Hoff and R. Perez, "Quantifying PV power output variability," Solar Energy, vol. 84, no. 10, pp. 1782–1793, 2010.
[34] M. M. Bandi and J. Apt, "Variability of the wind turbine power curve," Applied Sciences, vol. 6, no. 9, p. 262, 2016.

8. Appendix A- System Data and Probabilistic Model Parameters

8.1. Appendix A.1 – Load and Generator Data

Table A.1. AC and DC load demands at system buses

Bus No.	AC Loads		DC Loads
	P_L^{ac} (MW)	Q_L^{ac} (MVAR)	P_L^{dc} (MW)
1	-	-	-
2	1.00	0.45	-
3	-	-	1.25
4	0.5	0.25	-
5	0.5	0.25	0.5
6	0.75	0.35	0.75
7	0.50	0.25	-
8	0.50	0.25	1.25
9	-	-	0.85
10	0.50	0.25	0.50
11	-	-	-
12	-	-	1.25
13	0.75	0.35	-

Table A.2. Data for the system generators

DG No.	DG Type	P_G^{max} (MW)	P_G^{min} (MW)	Q_G^{max} (MVAR)	Q_G^{min} (MVAR)
G1	DSS, AC	10.0	1.0	4.80	0.8
DG4	PV, DC	1.50	0	0	0
DG7	PV, DC	1.50	0	0	0
DG9	Wind, AC	1.00	0	0	0
DG11	PV, DC	1.50	0	0	0
DG13	Diesel DG, AC	2.00	0.2	0.96	0.1

8.2. Appendix A.2 – Probabilistic Model Parameters

Table A.3. PDF parameters for each stochastic model

Load Demand	Winter	$k = -2.0498,\ \sigma = 76.5706,\ \mu = 33.8229$
	Spring	$k = -2.0299,\ \sigma = 64.7435,\ \mu = 30.9216$
	Summer	$k = -2.1535,\ \sigma = 123.2435,\ \mu = 43.8349$
	Fall	$k = -2.0299,\ \sigma = 60.6328,\ \mu = 28.9583$
PV Power	Winter	$\gamma = 0.6561,\ \delta = 0.1853,\ \lambda = 30.5430,\ \xi = -0.4102$
	Spring	$\gamma = 0.4549,\ \delta = 0.2182,\ \lambda = 81.8414,\ \xi = -1.3103$
	Summer	$\gamma = 0.4199,\ \delta = 0.2332,\ \lambda = 96.1342,\ \xi = -1.6687$
	Fall	$\gamma = 0.6052,\ \delta = 0.2301\ \lambda = 59.0836,\ \xi = -1.0902$
Wind Power	Winter	$\gamma = 1.4584,\ \delta = 1.6624,\ \lambda = 32.9295,\ \xi = 80.6751$
	Spring	$\gamma = 0.1402\ \delta = 0.6340,\ \lambda = 25.9017,\ \xi = 30.9977$
	Summer	$\gamma = 0.3993\ \delta = 0.3682,\ \lambda = 28.1423,\ \xi = 13.8442$
	Fall	$\gamma = 0.7441\ \delta = 1.6674,\ \lambda = 43.7649,\ \xi = 7.0870$
EV Station	All Seasons	$\gamma = -0.1555\ \delta = 0.4199,\ \lambda = 94.1582,\ \xi = -4.1414$

Note: For Johnson SB distribution, parameters are γ (shape 1), δ (shape 2), λ (scale), and ζ (location). For Generalized Pareto distribution, parameters are k (shape), σ (scale), and μ (threshold).